Nature Communications

https://doi.org/10.1038/s41467-026-69589-5

Article in Press

Satellite mapping of every building's function in urban China reveals deep built environment disparities

Received: 29 August 2025

Accepted: 29 January 2026

Cite this article as: Li, Z., Li, L., Hu, T. *et al.* Satellite mapping of every building's function in urban China reveals deep built environment disparities. *Nat Commun* (2026). https://doi.org/10.1038/s41467-026-69589-5

Zhuohong Li, Linxin Li, Ting Hu, Mofan Cheng, Wei He, Tong Qiu, Liangpei Zhang & Hongyan Zhang

Satellite mapping of every building's function in urban China reveals deep built environment disparities

Zhuohong Li[1,2,†], Linxin Li[1,†], Ting Hu[3,†], Mofan Cheng[1], Wei He[1], Tong Qiu[2,*], Liangpei Zhang[4,1,*], and Hongyan Zhang[5,*]

[1]State Key Laboratory of Information Engineering in Surveying, Mapping, and Remote Sensing, Wuhan University, Wuhan, Hubei, 430079, PR China
[2]Nicholas School of the Environment, Duke University, Durham, North Carolina, 27708, USA
[3]School of Remote Sensing and Geomatics Engineering, Nanjing University of Information Science and Technology, Nanjing, Jiangsu, 210044, PR China
[4]Aerospace Information Research Institute, Henan Academy of Sciences, Zhengzhou, Henan, 450046, PR China
[5]School of Computer Science, China University of Geosciences, Wuhan, Hubei, 430074, PR China
[†]These authors contributed equally: Zhuohong Li, Linxin Li, Ting Hu
[*]corresponding authors: Tong Qiu (tong.qiu@duke.edu), Liangpei Zhang (zlp62@whu.edu.cn), Hongyan Zhang (zhanghongyan@cug.edu.cn)

Abstract

Decades of rapid urbanization have reshaped China's cities, yet fine-scale built environment disparities remain unclear due to scarce building-level data. Here, we present SinoBF-1, a national building functional map of China that delineates 110 million buildings across 109 major cities using 1-meter multi-modal satellite data. Using nine indicators spanning urbanization intensity, facility accessibility, and infrastructure sufficiency, we quantify disparities across city tiers, geographic regions, and intra-city zones. Analyses reveal that: (1) Across city tiers, accessibility and amenity diversity decline sharply from top- to low-tier cities, while mid tiers show more equitable housing allocation; (2) Geographically, southern cities exhibit the highest access to healthcare, education, and public services but suffer from infrastructure overcrowding; and (3) Within cities, later-expanding zones exhibit greater disparities than early-established urban cores. This study reflects legacies of national development policies over the past half-century and offers a framework for evaluating urban inequality in rapidly urbanizing regions.

Introduction

Cities—home to more than half of the global population—serve as major engines of socio-economic development and generate 80% of the world's gross domestic product (GDP)[1]. Nowhere is this urban dynamism more evident than in China, where four decades of rapid urbanization, driven by reform and opening-up policies, have transformed the nation into a global economic powerhouse, contributing one-fifth of the world's GDP and hosting 66% of its population in cities[2]. Yet beneath this growth lies a deep and persistent spatial disparity[3]. Despite massive investments, industrialization, and modernization, cities across China exhibit striking disparities in livability, access to infrastructure, and economic opportunity[4]. Although administrative city tiers are not standardized metrics of urban form or function, they serve as a practical proxy for China's urban hierarchy, where higher-tier cities have historically received greater policy support and infrastructure investment than lower-tier counterparts[5]. Geographically, the 1935-proposed “Hu Huanyong Line” divided China into two contrasting parts, where the southeastern part with 43% of China’s total area carries 94% Chinese population and produces 95.7% of China’s GDP[6]. National policies, such as the “Northeast Industrial Revitalization Plan”[7], were introduced to mitigate enduring scars of inequalities brought by historical legacies of war preparedness and industrial relocation[8]. These geographic and socio-economic disparities undoubtedly challenge equal residential environments across China. The inequalities that manifested in resources[9], facilities[10], housing[11], etc., threaten long-term socio-economic advancement and harm sustainable development[12,13]. However, efforts to monitor and understand urban disparities have been hampered by the absence of fine-scale, nationwide data and by the lack of comprehensive frameworks capable of capturing the multi-dimensional nature of disparities. Here, we overcome both limitations and present a national-scale building functional map of China (SinoBF-1), covering 110 million buildings. Our results revealed a systematic, multi-dimensional disparity spanning urbanization intensity, facility accessibility, and infrastructure sufficiency. Our analysis provides a valuable framework that situates today’s patterns in their policy legacies, contributing to the ongoing discourse on inequality in the built environment.

As the most granular units of urban form, buildings are the foundational elements of both residential life and economic activity. Their spatial distribution and functional composition directly shape the fabric of cities[14] . Understanding the attributes of individual buildings is therefore essential for capturing the fine-scale structure of urban environments and the inequalities embedded within them[15]. Advances in high-resolution satellite imagery now offer an opportunity to observe cities at the scale of individual buildings[16,17]. To date, most building-level studies have focused on geometric attributes, such as footprint, height, and density, to evaluate their effects on transportation systems[18], public health[19], and energy use[20]. Many studies of building footprints or rooftop mapping have achieved significant success at a global scale[21,22]. However, while we now know where buildings are and how they are distributed, we still know remarkably little about what individual buildings are used for. This functional blind spot represents a critical limitation in current urban research. Recent effort has developed a dataset that provides functions for 31 million buildings[23] in China, yet research in this field remains at its early stages, severely constraining our ability to analyze national-scale disparities using fine-grained building functions and resource distribution.

Numerous studies have sought to assess disparities in the built environments, yet most have been constrained by coarse spatial resolution and a narrow, single-dimensional focus. For instance, global-scale travel-time maps at a 1-km resolution have been used to measure accessibility as a proxy for resource disparities[24]. Similarly, unequal allocation in infrastructure[25], public services[26], green spaces[27], and household water[28] have been evaluated using low-resolution grids ($\geq$ 200 m) or aggregated statistical data—each study addressing isolated dimensions in fragmented ways. These unidimensional approaches, though insightful, fall short in capturing the complexity of spatial disparities, which are inherently multi-faceted and spatially heterogeneous. As a result, current knowledge is limited in both resolution and scope, leaving many critical indicators and their interactions underexplored. Addressing this gap requires a paradigm shift toward high-resolution and multi-dimensional assessments that can reveal the full extent and structure of urban disparity.

A multi-level system is also needed to understand how spatial disparities unfold within China's unique socio-institutional context. First, the city tiers reflect China's administrative and economic hierarchy, shaping how resources are distributed among cities[29]. Second, geographic regions capture historical and environmental divides —the coastal–inland gradient—that continue to structure disparities in development and population[4]. Finally, intra-city zones reveal differences between early established urban cores and later-expanding urban zones, where residents directly experience unequal access to infrastructure and services.

Here, we present SinoBF-1[30], a national-scale building functional map of China derived from more than 69 terabytes of multi-source satellite data, including optical imagery, nighttime lights, and altimetry observations. This fine-grained dataset captures the attributes and functions of approximately 110 million buildings across 109 cities, covering a total area of 1,094,344 km^2. To systematically assess residential inequality and its drivers, we introduce a multi-dimensional framework[31] comprising nine fine-scale indicators that are closely associated with the built environment and residents' daily lives (see Supplementary Table 1). They are grouped into three core dimensions: urbanization intensity, facility accessibility, and infrastructure sufficiency. Each assessment dimension is explained as follows: (1) Urbanization intensity is represented by building height, density, and nighttime light intensity; (2) Facility accessibility is quantified by the travel time from each residential building to the nearest education, healthcare, and public service facilities, reflecting residents' access to essential urban services; (3) Infrastructure sufficiency captures the diversity and adequacy of local urban form, using metrics of neighborhood amenity diversity, housing inequality, and per capita infrastructure occupation. We then address how institutional, geographical, and local mechanisms shape patterns of disparities across the urban landscape by answering two questions: (1) What are the national patterns of building function across China's urban landscape? (2) How do disparities in the residential built environment vary across city tiers, geographic regions, and intra-city zones? By addressing them, this study provides a lens to understand the structure of disparities in rapidly urbanizing contexts. This approach establishes a scalable way for assessing global urban development's spatial inequality, helping design more equitable, inclusive, and sustainable cities.

Result

Overview of building function distributions in urban China

To classify the functions of buildings, we define eight building categories according to the construction classification standards of China. These include residential, commercial, administrative, healthcare, sport and art, educational, industrial, and public service. Representative examples and visual legends are presented in Fig. 1a. According to China's city hierarchical system, there are five city tiers which reflects decreasing gradients of political influence, economic activity, industrial capacity, and population size from Tier 1 to Tier 5[29]. We selected 109 cities that cover all city tiers and geographical regions, accounting for about half of China's population and 70% of its GDP (Fig. 1b, Supplementary Fig. 1). To assess the reliability of our building-level functional classification, we conducted validations at the statistical, building, and point levels using two independent sources: (1) official government reports from the National Bureau of Statistics[32] and the Ministry of Housing and Urban-Rural Development of China[33]; (2) large geospatial reference point sets comprising 5,280,695 field observation samples from Amap Inc. As shown in Supplementary Fig. 2a and Supplementary Table 2, the resulting functional map achieved strong agreement with external benchmarks, with an average R^2 of 0.8208 at the statistical level and an overall accuracy of 84.65% at the individual building level (see method for details).

Analysis of the national building function (Fig. 1c, Supplementary Fig. 2b) reveals a clear alignment between urban functional structure and economic specialization of cities in GDP compositions across tiers[34]. Higher-tier cities, particularly Tier 1 and Tier 2, are characterized by a greater prevalence of commercial buildings, reflecting the dominance of service-based economies. For example, Macau, a Tier

2 city in southern China, exhibits the highest proportion of commercial buildings among all cities analyzed (36.81%), reflecting its exceptional service-oriented economy in which the tertiary sector accounted for 92.26% of GDP in 2021. In contrast, Tier 5 cities in the southwest show a predominance of industrial buildings, indicating their manufacturing- and resource-based economic structures. Panzhihua, a major hub for steel, vanadium, titanium, and energy production, recorded the highest share of industrial buildings (54.1%), with the secondary sector comprising 54.8% of its GDP.

We assess the residential built environment across 109 cities using nine building-level indicators grouped into three key dimensions: urbanization intensity, facility accessibility, and infrastructure sufficiency (Fig. 2). Together, these indicators enable a multi-dimensional evaluation of spatial disparities at a fine scale. In the following sections, we apply this framework to examine how disparities manifest across China's urban hierarchy—first among city tiers, then across broad geographic regions, and finally within individual cities.

Urban Disparities Along China's City Hierarchy

Urbanization intensity (Fig. 2a), as captured by building height, density, and nighttime light intensity, varies systematically across China's city tiers, yet reveals notable and unexpected patterns (Fig. 3a). The distribution of building height in Tier 2 cities shows a surprising deviation: the mode value is the lowest among all tiers (10 meters). By contrast, Tier 2 cities exhibit the highest average building density across all tiers, where the representative city, Zhengzhou (Fig. 1b), stands out as the most spatially compact city, with a density exceeding 400 buildings per km^2. This suggests that Tier 2 cities, despite their economic significance, may favor horizontally expansive development over vertical growth. These patterns indicate that density and height—though often correlated—may follow divergent trajectories depending on development strategy and planning constraints at the tier level. Overall, the results show that Tier 1 cities have the tallest buildings, but the differences among tiers remain relatively modest, ranging from 13 m to 10 m. In the building density, Tier 2 cities exhibit a slightly higher density than Tier 1, while both are substantially higher than the other tiers.

Facility accessibility was evaluated using the high-resolution map that integrates our building functions with a hierarchical traffic network and 1-meter land-cover product that we previously produced (Supplementary Fig. 3). This map quantifies the minimum travel time required for each residential building to reach its nearest education, healthcare, and public services (Fig. 2b, 3b). Tier 1 cities exhibit markedly higher accessibility. Over 78% of residential buildings in Tier 1 cities are within a five-minute walk of the nearest education facilities, compared to 22% in Tier 5 cities. Similar disparities are observed for healthcare (52% vs. 28%) and public service (47% vs. 16%). In Tier 5 cities, more than 70% of residents must travel over 15 minutes to access at least one of these essential facilities. Furthermore, similar accessibility patterns were observed using either population or residential buildings on the y-axis, with Tier 1 and 2 residents reaching facilities substantially faster than those in lower-tier cities. The accessibility maps across five representative cities (Fig. 3c, Supplementary Fig. 4) further reveal a consistent pattern: areas with high population density tend to coincide with zones of high facility accessibility.

Infrastructure sufficiency, the third dimension to evaluate spatial disparities in cities, reveals substantial variations across city tiers (Fig. 4). The first indicator, neighborhood amenity diversity, captures both the richness and availability of six facility types (e.g., commercial, sport and art, etc.) within 15-minute walking zones. Tier 1 and 2 cities cluster in the high-diversity, high-availability quadrant of Fig. 4a. In contrast, the majority of Tier 4 and 5 cities fall in the low-diversity, low-availability quadrant, reflecting more limited neighborhood amenity diversity. The second indicator, housing inequality, is quantified using the Gini coefficient (see method for details), offering a proxy for equity in housing volume across the population (Fig. 4b). Tier 3 cities exhibit the lowest median disparity (0.56), outperforming Tier 1 and 2 cities. These results suggest that moderately developed cities may offer more equitable living conditions, despite having fewer total resources. The third indicator measures per capita occupation of healthcare and public service, reflecting the adequacy of infrastructure supply relative to local demand (Fig. 4c,d). Metropolises like Shanghai report the highest per capita provision overall. Conversely, major Tier 1 cities such as Shenzhen and Guangzhou exhibit lower-than-expected healthcare space per person, trailing behind many Tier 3 and 4 cities. Together, these findings challenge the assumption that infrastructure sufficiency scales directly with economic development. While metropolises are often presumed to offer more equitable amenities, our analysis reveals that mid-tier cities can outperform higher-tier cities. These patterns highlight the potential advantages of moderately developed urban systems.

Uneven development across China's geographic regions

China's residential built environments also exhibit deep regional disparities, shaped by long-standing imbalances in population distribution, economic development, and infrastructure investment[3]. In terms of facility accessibility (Fig. 2b, Supplementary Fig. 2c), the southern and eastern regions consistently demonstrate the highest accessibility to educational, healthcare, and public services, reflecting more integrated urban facilities. Central and northern regions show particular strength in educational accessibility, supported by resource-rich cities like Wuhan and Beijing[35]. In contrast, the northwestern regions face substantial deficits in facility access, especially for healthcare and public services.

Regional patterns of infrastructure sufficiency echo these divides (Fig. 2c). The eastern region reports the highest neighborhood amenity diversity, with a Shannon entropy index of 0.76 (Fig. 4a, Supplementary Fig. 5c), while the northwest lags far behind at 0.27, indicating a more monotonous and insufficient facility landscape. Housing inequality also varies markedly: the northern and northeastern regions show the greatest disparities in residential capacity allocation, despite having the highest proportion of residential buildings (84.06% and 83.97%, respectively). Cities like Hohhot and Anshan exhibit the most unequal distributions, with Gini coefficients of 0.77 and 0.74, respectively. By contrast, the southern region demonstrates the most equitable housing distribution, with an average inequality index of 0.54. However, equity in housing is not necessarily related to adequate infrastructure provision. Southern cities generally face more overcrowded public infrastructure, with per capita space for healthcare and public services averaging just 0.006 m^2 and 0.031 m^2, respectively—substantially lower than values in central, eastern, and northern regions (Fig. 4c,d). Northwestern cities, meanwhile, confront compounded challenges of both limited facility access and low functional diversity (Fig. 2c), reinforcing spatial disadvantage across multiple dimensions.

Built environment disparities within cities

To evaluate spatial disparities within cities, we further divided each studied city into three zones—urban core, intermediate zone, and urban periphery—based on their development stage, functional planning, and administrative boundaries. This zoning approach enables a consistent comparison of infrastructure and service disparities across urban gradients. As a typical sample illustrated in Fig. 5a, the delineation of zones in Beijing shows distinct population concentrations. In the assessment, we focused on facility accessibility (Fig. 5b) and infrastructure sufficiency (Fig. 5c) because the first dimension (i.e., urbanization intensity) is inherently defined at the city-wide scale rather than intra-urban zones.

In terms of facility accessibility, urban cores consistently offer the shortest travel time to essential facilities. On average, residents in urban cores reach education, healthcare, and public service facilities within 15, 9, and 18 minutes, respectively. In contrast, those in intermediate zones face substantially longer travel time—43, 24, and 51 minutes—while residents in urban peripheries endure the heaviest travel burdens, requiring 69, 37, and 83 minutes, respectively, to access these functional buildings. These patterns reflect a classic core–periphery structure, consistent with global urban trends[26], and highlight the persistent service accessibility challenges faced by populations in expanding peripheral zones.

With regard to infrastructure sufficiency, our analysis challenges the common assumption that intermediate zones represent sites of future urban advantage[36]. Instead, we find that these zones exhibit the highest disparities in residential capacity allocation, with a Gini coefficient of 0.56—compared to 0.41 in urban cores and 0.54 in urban peripheries. Meanwhile, peripheries that typically have lower population densities report the highest per capita public infrastructure provision (0.18 m^2), exceeding both urban cores (0.16 m^2) and intermediate zones (0.10 m^2). This suggests that while peripheral areas may benefit from lower demand, intermediate zones are marked by both high population pressure and insufficient infrastructure expansion. To further compare the effects of different intra-city regional division methods on the results, we attempted to delineate these areas based on population and building density, and the results showed strong consistency. The overall assessments of infrastructure sufficiency indicate that urban cores continue to offer the most well-resourced residential environments, largely due to their early development and historic concentration of facilities[37]. Despite targeted planning initiatives aimed at rapidly developing intermediate zones[38], these areas still suffer from overcrowded infrastructure (low per capita allocation) and housing problems (high inequality index).

Discussion

This study offers a previously unavailable, high-resolution perspective on spatial disparities across urban China by linking building-level functional classifications with multi-dimensional indicators of urbanization intensity, facility accessibility, and infrastructure sufficiency. By mapping and quantifying disparities across city tiers, geographic regions, and within cities themselves, we uncover spatial structures of disparities that were not detectable using conventional, coarse-scale data. In the following parts, we interpret these findings in the context of major national development strategies over the past half-century—demonstrating how state-led policies have shaped, and in some cases intensified, spatial disparities in urban China.

Our analysis reveals distinct patterns in building function distributions across both city tiers and geographic regions, shaped in part by legacy national development policies. In particular, we find that the spatial allocation of industrial buildings strongly reflects the influence of the "Third Front Movement", a strategic government initiative launched in the 1960s to relocate heavy industries to inland southwestern cities for national defense purposes[8]. Over the past six decades, this industrial transfer has contributed to the economic stagnation of northeastern China, where many state-owned enterprises were originally located and later downsized or relocated[39]. While previous studies have documented high vacancy rates in residential housing in northern China[20], our study provides spatially explicit evidence that residential buildings now overwhelmingly dominate the built environment in northern and northeastern cities (Supplementary Fig. 2b). These regions also exhibit the sparsest distribution of educational facilities—nearly half the density observed in central and eastern cities—and continue to show the lowest per capita GDP and the highest shares of primary industry in their economic composition. Although revitalization efforts such as the "Northeast Industrial Revitalization Plan" were introduced in the early 2000s[7], our building-level assessment shows that foundational infrastructure in these cities continues to lag behind. Furthermore, we also find significant disparities across city tiers. Low-tier cities contain disproportionately high concentrations of industrial buildings, while the share of commercial buildings increases steadily with tier level (Fig. 1c). These divergent functional structures imply systematic differences in economic orientation and urban livability, which may contribute to ongoing population loss and internal migration from lower-tier cities—trends that align with observed urban mobility patterns reported in previous studies[3,12].

A clear core–periphery gradient in facility accessibility emerges within Chinese cities, consistent with global observations of urban disparities. We find from building-level attributes that residents in urban cores consistently enjoy the shortest travel times to essential facilities, while those in intermediate zones and peripheries face substantially higher time costs (Fig. 5b). This pattern aligns with prior findings at coarser resolutions in global metropolises[24,26], but our results provide a more granular and systematic view across 109 cities. By moving beyond large cities and incorporating underdeveloped areas, we uncover far more pronounced disparities than previously reported. At the national scale, facility accessibility varies sharply across both city tiers and geographic regions. Although previous studies have primarily investigated the healthcare accessibility in China[40,41], our analysis reveals that severe inequalities also exist in access to education and public services. For public services, the modal travel time in Tier 5 cities is 25 minutes—more than sevenfold higher than the 3.5 minutes observed in Tier 1 metropolises (Fig. 3b). The typical time of northwestern cities to reach public services is six times longer than in southern China (24 vs. 4 minutes). In response to these challenges, the government introduced the "Western Land-Sea New Corridor Plan" in 2019 to improve infrastructure in northwestern cities[42]. Our findings suggest that efforts to enhance public service and healthcare accessibility should be prioritized as part of China's broader strategy to alleviate disparities among tiers and regions.

This study introduces an approach for evaluating infrastructure sufficiency by measuring both the diversity and adequacy of infrastructures. The fine-grained building-level details allow us to uncover disparity patterns that remain hidden in conventional gridded or administrative datasets[26]. Our results show that neighborhood amenity diversity is highly stratified by city tier and geography. Tier 1 cities exhibit, on average, four times greater amenity diversity than Tier 5 cities (Fig. 4a), while eastern cities show great advantages over northwestern counterparts (Fig. 4a, Supplementary Fig. 5). Our results move beyond prior global-scale assessments of infrastructure disparities[25,43] by revealing how disparities in both diversity and adequacy are embedded at the scale of individual buildings. For example, residents in Tier 1 cities benefit from dramatically more infrastructure: per capita public service space is eight times larger than in Tier 5 cities (Fig. 4c), while healthcare provision shows a fivefold difference (Fig. 4d)—inequities that remain obscured in aggregate-level analyses[25,43]. Furthermore, we find that housing equity does not increase linearly with city development. Instead, residential capacity allocation exhibits a U-shaped trajectory across tiers, with Tier 3 cities demonstrating the lowest disparity index (Fig. 4b). This trend aligns with prior findings on land carrying capacity[44] and housing affordability[45], but our study further shows how this pattern manifests at a building level through China. Regionally, housing inequality is most pronounced in northern and northeastern cities, while the most equitable conditions appear in the south (Fig. 4b)—consistent with prior county-scale patterns[29]. While previous social surveys have revealed broad trends in infrastructure disparity across China[46], they lack the resolution to identify where and how these disparities emerge.

Our findings underscore the need to examine spatial disparities in cities as a multidimensional system, rather than through isolated indicators. By quantifying disparities in facility accessibility and infrastructure sufficiency, and synthesizing them into a composite score, our study provides a comprehensive picture of the residential experience in China (Fig. 5d,e, Supplementary Table 3). Despite persistent challenges like housing inequality, metropolises consistently score highest in overall residential conditions. These advantages are likely driven by the concentration of high-quality infrastructure, but may also intensify demand and exacerbate residential space scarcity. This divergence suggests that high urban livability may coexist with mounting spatial pressures at the building scale. Regionally, we observe a spatial divide that mirrors the 1935-proposed "Hu Huanyong Line"[6], with eastern and southern coastal cities largely outperforming their western and northern counterparts across most indicators, which corroborates the long-term, historical development pattern and reveals the disparity drivers of Chinese geographic regions.

Our results reveal coherent patterns across scales and indicators. Urban cores and higher-tier cities in the eastern and southern regions exhibit shorter travel times and greater amenity diversity, whereas lower-tier cities in the northern and western regions and later-expanding urban areas show poorer accessibility and lower diversity. Divergences are equally informative. Mid-tier cities display more equitable housing allocation than top tiers, and Tier-2 cities combine the highest building density with the lowest modal height, indicating a density–height decoupling. Urbanization intensity generally co-varies positively with facility accessibility and with amenity diversity, but relates negatively to per-capita infrastructure provision. These cross-scale relationships underscore how urbanization drives spatial disparities in Chinese cities.

This study offers a nationwide and building-level evaluation of spatial disparities of urban China, but two key limitations warrant consideration. First, while our analysis captures fine-grained spatial disparities in infrastructure, services, and residential patterns, it does not directly incorporate socioeconomic attributes of individuals or households (e.g., income, occupation, or service usage). As such, our results reflect spatial disparities in the built environment rather than comprehensive social inequality. Future work could extend this framework by integrating household-level survey data or administrative statistics to assess how spatial patterns align with socioeconomic outcomes. Second, although our building function classifications were derived from well-established datasets, they inevitably inherit uncertainties from partial volunteer-contributed data (e.g., OpenStreetMap)[47–49]. In the mapping process, we have undertaken a sample selection and extensive validation efforts to mitigate and assess the impact of these uncertainties on the results.

This study reframes the understanding of disparities in built environments and demonstrates how they are spatially structured and vary across tiers, regions, and intra-urban areas. This is a nationwide study to uncover hidden layers of building-level disparity that remain invisible in previous studies. Our findings demonstrate that building-scale indicators can capture subtle yet systematic differences in infrastructure access and diversity, revealing spatial gradients that were invisible in coarse-scale national surveys or aggregate socio-economic data. In doing so, the study advances not only urban science but also the tools available to planners and policymakers: the framework we propose is scalable, transferable, and aligned with global efforts to monitor progress toward SGDs. Beyond China, this approach offers a replicable model for diagnosing spatial disparity in rapidly urbanizing regions where detailed administrative data may be unavailable. It also opens up research avenues linking the built environment to environmental exposure, climate risk, health outcomes, and social mobility.

Methods

The overall workflow of this study encompasses two key parts: (1) national-scale building function mapping and validation; (2) multi-level assessments of residential built environments. This section comprehensively explains the data sources, the proposed mapping models, and the assessment indicators. In Supplementary Figs. 6 and 7, we demonstrate the details of the workflow and main operations. By integrating these elements, we aim to provide an overall workflow for building-scale mapping, validation, and residential built environment assessment.

Data

To comprehensively characterize building attributes and identify their functions, we utilized three modalities of satellite data as mapping sources, where Supplementary Fig. 8 illustrates the typical samples of each data. First, to capture fine-scale building appearances, we acquired high-resolution ($1.07m/pixel$) optical images from Google Earth imagery. By integrating imagery from advanced sensors and satellites, Google Earth imagery emerges as a freely accessible high-resolution data source with complete coverage of China. The cloud-free and high-quality imagery, produced through advanced pre-processing by Google Earth, makes it a suitable source for fine-scale building observation[50]. Second, to describe the stereoscopic attributes of buildings, we used the 10-m resolution building height data of China (CNBH-10m)[51]. The CNBH-10m, as the finest available building height dataset covering China, is generated through data fusion from Sentinel-1 and -2, PALSAR, LuoJia 1-01 satellites, and settlement footprint data, providing critical information on building verticality. Third, to assess nighttime production activities and potential energy consumption patterns, we incorporated 10-m resolution nighttime light images from the SGDSAT-1 satellite platform. As an advanced scientific satellite dedicated to SDGs[52], SGDSAT-1 was launched in 2021 and equipped with a glimmer imager, a multispectral imager, and a thermal infrared spectrometer. This dataset offers a perspective on urban activity levels and energy use at a high spatial resolution, further enriching our understanding of building functionality.

To make better use of these data, we performed preprocessing on the input data to mitigate the potential impact of imaging noise on building function mapping. The procedure is illustrated in Supplementary Fig. 6. We first resampled the building height data and nighttime light data to 1.07 meters per pixel based on the resolution of the optical imagery. Then, following previous processing workflows, we selected cloud-free or thin-cloud scenes from the SGDSAT-1 nighttime light imagery, then we performed stripe noise removal and radiance correction to mitigate the effects of imaging noise[53,54]. Furthermore, all three raster modalities were in the geographic coordinate system of WGS 1984. To ensure stricter spatial correspondence among them, we performed co-registration on the input raster data. Supplementary Fig. 8 (a)–(c) shows the three processed input rasters. Finally, the processed multi-modal remote-sensing data were concatenated at the band level to form an aligned data cube for input into the deep learning model.

Besides, to assess the facility accessibility across 109 cities, the national-scale 1-meter resolution land-cover map of China (SinoLC-1) that was produced in our previous study[55] and hierarchical traffic networks from the OpenStreetMap were utilized as the auxiliary data. By combining these data sources with the produced building function map of this study, we were able to robustly calculate the travel time consumption between each residential building and other functional facilities to produce the 1-meter-resolution, building-scale accessibility maps, ensuring a comprehensive and reliable analytical procedure.

Furthermore, to generate stable and reliable labels of building footprint and function information, we leveraged four types of open-access datasets. First, to define the precise boundaries of China's building footprints, we utilized the CN-OpenData dataset[56], which provides detailed building locations and boundaries for 90 major cities in China. To further supplement footprint annotations, we incorporated data from the East Asia Building Dataset[57], which serves as an auxiliary source for enhancing annotation coverage across China. Second, for building function annotations, we compiled labeled samples by integrating land-use and area-of-interest (AOI) data from OpenStreetMap, a widely recognized Volunteered Geographic Information (VGI) source. Although volunteer-contributed data may have classification or positional uncertainty, the accuracy and reliability of OpenStreetMap in China have been widely discussed and validated[47–49]. Many urban studies, both in China and globally, have used it as a critical data source for understanding urban patterns, applying it to discussions on urban sustainability, socioeconomics, transportation, and other aspects[24,58,59]. To accommodate the low noise-to-signal ratios in the OpenStreetMap labels, we further applied a weakly-supervised strategy in the model training protocol, screening for the reliable parts of the annotations. Together, these diverse data sources provided a comprehensive basis for accurate and detailed building function mapping at a national scale.

Lastly, to comprehensively evaluate the produced building function map, we incorporated a range of authoritative and high-quality datasets. Official government reports included the China Urban-Rural Construction Statistical Yearbook 2023 from the Ministry of Housing and Urban-Rural Development of China[33] and the China Statistical Yearbook 2023 from the National Bureau of Statistics[32], which were utilized as the statistical validation set. Furthermore, we employed 5,280,695 field-observed points of interest (POI) from Amap Inc. to conduct comprehensive validation at the building level. These POIs were collected by field survey volunteers or building owners, encompassing more than 100 subcategories of real-life facilities (e.g., supermarket, coffee shop, museum, and clinic). To align with the eight building functional types of this study, we further merged these subcategories following the classification guidelines provided by Amap Inc. Supplementary Tables 2 and 4 present the function definition, samples of these subcategories, and the class merging reference.

Deep learning-based mapping workflow

To accurately identify the 110 million buildings' functions involved in 109 cities, we designed an efficient mapping framework referring to our previous studies on national-scale fine-grained mapping in China. Specifically, the workflow contains data preprocessing, GeoAI model training and inference, and post-processing.

As shown in the first step of Supplementary Fig. 6, the data preprocessing systematically integrates multi-modality satellite imagery and multi-source annotation data to construct robust training pairs for the deep learning model. Initially, we combined three spectral bands of high-resolution optical images, one building height band, and three bands of nighttime light data into a high-dimensional data cube. Prior to integration, the height and nighttime light bands were normalized to [0, 1] using min–max scaling, and the optical bands were standardized via z-score normalization to reduce illumination and seasonal effects. This fusion of data layers enables a comprehensive representation of each building. Subsequently, we unified over 100 categories of land-use and AOI data from OpenStreetMap into eight targeted building function categories, in alignment with China's national standards, including the Standard of Construction Classification (No. GB/T 50841-2013), Unified Standard for Civil Building Design (No. GB 50352-2019), and General Specifications for Civil Buildings (No. GB 55031-2022). Next, the building footprints were overlaid with the unified function labels to generate the building-scale training labels. For efficient data organization, each city was divided into multiple storage tiles, each measuring 6000 pixels × 6000 pixels.

On average, approximately 30% of the buildings within each tile were annotated with their functions, ensuring sufficient labeled data for model training.

To efficiently exploit the generated training data for large-scale building function mapping, we employed the advanced deep learning model, Paraformer, which was specifically designed for large-scale map updating with limited labels in our previous studies[60,61]. Paraformer is a weakly supervised deep learning model that integrates a shallow convolutional neural network (CNN) branch with a vision transformer (ViT) branch. Supplementary Fig. 7a demonstrates the details structures of each branch. The CNN branch is constructed by five serially connected resolution-preserving (RP) blocks that proposed in our previous study[61]. Each RP block contains parallel convolution layers with the sizes of 1×1, 3×3, and 5×5, whose steps are set to 1 for feature size maintenance. This structure allows the CNN branch to capture fine-grained building features. For the ViT branch, which contains 12 transformer layers, leverages its global modeling capabilities to establish long-range dependencies among dispersed geographic areas. This dual-branch architecture enables the model to effectively handle the complex spatial heterogeneity of city environments. The semi-supervised training strategy further enhances the model's ability to learn from the 30% reliable labeled samples. In detail, we modify the cross-entropy (CE) loss by considering the background and all function types as the supervised classes. Then, building objects without function-labeled information is regarded as unsupervised classes, which are ignored during loss calculation. Formally, for a training patch of the size of $W \times H$, we used $\mathbf{Y}'$,$\hat{\mathbf{Y}}$, and $\mathbf{G}$ to represent the labels, results, and the unlabeled building mask, respectively. The modified CE loss can be written as:

$$\mathscr{L}_{MCE}(\mathbf{Y}', \hat{\mathbf{Y}}, \mathbf{G}) = \frac{-\sum_{i=0}^{W}\sum_{j=0}^{H}\left[g_{ij}\sum_{l=1}^{L} {y'}_{ij}^{(l)}\log(\hat{y}_{ij}^{(l)})\right]}{\mathrm{Sum}(\mathbf{G}(i,j)=1)}, \tag{1}$$

where ${y'}_{ij}^{(l)}$ and $\hat{y}_{ij}^{(l)}$ denote the pixel (i, j) of the label $\mathbf{Y}'$ and prediction $\hat{\mathbf{Y}}$ with the class l. If the pixel is a building object without function-labeled information, the g_{ij} is set to 0; otherwise, the g_{ij} is set to 1. To account for regional variations in building attributes and urban layouts across China, seven separate models were trained for each geographic region, following the training approach adopted in our previous national-scale mapping study[55]. During training, each data tile—comprising an aligned data cube and labels with sizes of 6000 pixels × 6000 pixels—was randomly cropped into 500 patches of 224 pixels ×

224 pixels. This approach maximized the use of training data while maintaining computational efficiency. A sample of the mapping result and the corresponding three-dimensional map are shown in Supplementary Fig. 8d,e. For model inference, a seamless mapping process was implemented. Input data cubes were assigned to their corresponding region-specific models, and a 112-pixel overlap was introduced between patches (224 pixels × 224 pixels) to mitigate edge artifacts. The resulting patches were then merged and seamlessly spliced to generate an intact and coherent building function map for each city. In general, this workflow ensured accurate, high-resolution mapping while addressing the challenges posed by the dense and diverse urban environments.

In addiction, we conducted a post-processing step to further optimize map products (see third step of Supplementary Fig. 6). In detail, this part was designed to vectorize the original building function map from raster format to polygons and supplement the building footprints that were incompletely mapped by the model. For every building footprint in the dataset, we first calculated the percentage area occupied by each functional type. If a particular functional type was found to cover more than 50% of the building's total area, we assigned that type to the entire building footprint. Buildings for which no single functional type occupied more than 50% of the footprint area were labeled as "unmapped", indicating that their functions could not be confidently determined due to mixed or incomplete class coverage. Subsequently, a lightweight classifier with Mask R-CNN structure[62] was employed to categorize unmapped building footprints. Supplementary Fig. 7b further delineates the details of the post-processing step. The structure contains: (1) the geo-prior encoder comprising a fully connected (FC) layer, a rectified linear unit (ReLU), and a dropout function; (2) the optical encoder comprising a ResNet50 backbone, a feature pyramid network (FPN), and a region of interest (ROI) align function. Following a strategy similar to the SEASONet method[?], we provided bounding boxes of the building footprints as priors, enabling the model to infer their categories with greater precision. Each building footprint was represented by its bounding box coordinates normalized to the image space, where the top-left corner corresponds to (0, 0) and the bottom-right corner to (1, 1). These normalized coordinates were fed into the geo-prior encoder, enabling the model to infer their categories with greater precision. Finally, all building vectors were merged according to urban administrative divisions to create a cohesive and unified map.

Accuracy validation

Given the importance of accurate mapping for downstream analysis, we conducted a comprehensive evaluation using government reports and in situ validation data outlined in the Data Section. This evaluation comprised two parts. First, a statistical-level evaluation was performed for each city based on official reports from the China Urban-Rural Construction Statistical Yearbook and China Statistical Yearbook. According to the classification system of these statistical reports, eight types of building functions were grouped into four primary categories: "residential", "commercial and business facilities", "administration, public services, and municipal utilities", and "industrial manufacturing, logistics, and warehouse". Supplementary Fig. 2a presents the details of statistical validation results. Second, a building-level geospatial evaluation was conducted by using 5.28 million field-observed points from Amap Inc., which is the most widely used map application in China for daily navigation with its high accuracy and reliability. Based on that,point-level and building-level accuracies were calculated to compare the in situ points with the mapped buildings at the same location. Before the verification, we selected some POI anchor points confirmed through street view photos and field tours for manual confirmation. Overall, it shows that POIs are strictly aligned with the utilized remote sensing data under the same WGS 1984 projected coordinate system.

Moreover, Supplementary Fig. 9a,c present the detailed information of point sets that were used in both point-level and building-level validation, including the total number of points of each building functional type and each city. Supplementary Fig. 9b illustrates the spatial distribution of validation points in a sample area of Beijing. Specifically, Supplementary Fig. 9d demonstrates a typical example of the POI-based validation process. For point-level validation, each POI point is treated as the smallest verification unit. It is considered a correct sample if its assigned category matches the functional type of the building it belongs to; otherwise, it is an incorrect sample. For building-level validation, each building is treated as the smallest verification unit. If the majority of POIs within a building match its functional type (i.e., their number exceeds the total of all other POI types), the building's function is considered to be correctly identified.

From the above verification protocols, statistical-level verification reflects the city-scale consistency between the map product and the official government report. Based on the POIs, building-level verification reflects a more practical measure of product accuracy, since if most rooms or POIs within a building serve a particular function, it should be considered as the building's primary functional type. As a reference, we also calculated the point-level accuracy in a stricter way, which does not ignore or tolerate the inconsistent POIs (e.g., rooms or entities in the same building) serving different functions with the building type. In general, Supplementary Table 2 shows the classification system and accuracy of each functional type at the point, building, and statistical levels.

Multi-level residential environment assessment metrics

To examine the built environment qualities, the nine assessment indicators are grouped into three dimensions: urbanization intensity, facility accessibility, and infrastructure sufficiency.

Dimensions of urbanization intensity includes the building height, building density, and nighttime light intensity. For the building height, we utilized the 10-m resolution building height data of China, i.e., CNBH-10m, to extract every building's height across 109 cities. For the building density, we measured the total building amounts from the produced building function map and divided it by the total administrative area of the city. For the nighttime light intensity, we referenced the boundaries of the GAIA product[63] and the statistics of normalized nighttime light intensity (0–255) within those areas, adopting 30 as the threshold to indicate high-intensity human activity. Accordingly, we identified and quantified areas in the SDGSAT-1 nighttime light imagery where the intensity exceeded this threshold. Then, we calculated their proportion compared to the total urban area. Fig. 2a demonstrates the spatial distribution of these indicators.

Dimensions of facility accessibility indicates residents' ease in accessing specific services or facilities. In detail, there are three main steps to quantify the facility accessibility. (1) Cost matrix construction: based on Weiss's research on modeling the speed of individuals across the landscape[24], we integrated the previously produced land-cover product—SinoLC-1 and traffic network data—OpenStreetMap, assigning time-cost weights to each land use and road type to construct the cost matrix. The time-cost weights were collected from two well-established studies[24,64], and the weight values were shown in Supplementary Tables 5 and 6. (2) Facility accessibility calculation: to generate the facility accessibility maps, we obtained the CostDistance function, which calculated the least accumulated cost of each pixel to the nearest facility. (3) Building-level quantification: we calculated the average accessibility for each residential building to assess the inhabitants' facility accessibility. The spatial analysis tools utilized in this study were implemented using the WhiteboxTools geospatial data analysis platform[65]. Supplementary Fig. 10 presents several examples of the accessibility maps across 12 cities, while Supplementary Fig. 11 shows the acquisition dates of the high-resolution imagery used to produce the SinoBF-1 and SinoLC-1, which served as the basis for calculating these accessibility maps.

Dimensions of infrastructure sufficiency includes indicators of neighborhood amenity diversity, inequality of residence capacity allocation, and per capita infrastructure occupation, which aim to measure both the diversity and adequacy of infrastructures. The details of these indicators are explained in this section. Firstly, diverse neighborhood amenities provide a comfortable and adaptable living environment, addressing the challenges of growing population density and the need for sustainable urban development. Moreover, a neighborhood circle refers to a basic unit within walking distance that meets daily living needs[?]. We evaluated the neighborhood amenity diversity around residential buildings using a 15-minute walking distance (1 km buffer), following the Technical Guidelines for Community Life Circle Planning issued by the Ministry of Natural Resources of China[66], focusing on two indices: building availability and amenity diversity (Supplementary Fig. 5a,b). Notably, the calculation involves the building types of commercial, administrative, healthcare, sport and art, educational, and public service, where industrial buildings are excluded from the analysis as they contribute little to residential comfort. First, availability reflects the residential and other functional buildings' density within the 15-minute neighborhood circle[67]. For each residential unit k, the building availability was calculated as follows:

$$A_k = \sum_{i=1}^{n} \mathrm{NIF_i}, \tag{2}$$

where NIF represents the non-industrial amenity, and n is the number of these amenities. Second, amenity diversity signifies the richness and balance of infrastructures[68]. We utilized Shannon's index to quantify the amenity diversity, and the diversity of residential unit k was calculated as follows:

$$D_k = -\sum_{c=1}^{m} p_c \log p_c = -\sum_{c=1}^{m} \frac{n_c}{\sum_{c=1}^{m} n_c} \log \frac{n_c}{\sum_{c=1}^{m} n_c}, \tag{3}$$

where m is the number of categories of amenities, p_c and n_c represent the proportion and number of the living amenities within the 15-minute neighborhood circle, respectively.

Furthermore, adequate, safe, and affordable housing is a fundamental goal of sustainable urban development. Residence capacity allocation directly reflects the level of equality in urban living conditions[69]. To quantify this, we applied the Gini coefficient to measure inequality in the distribution of residential building space:

$$G = 1 - \sum_{t=1}^{T} (P_t - P_{t-1})(V_t + V_{t-1}), \tag{4}$$

where t denotes the rank in the cumulative percentage of the population and the building volume, sorted in ascending order by average building space per capita, P_t represents the cumulative proportion of the population, and V_t represents the cumulative proportion of residential building volume allocated by the corresponding group of people. For each grid cell containing multiple residential buildings, we estimated the population allocation to each building by multiplying its residential floor area with the population density of the grid cell, assuming a uniform distribution of residents across residential spaces.

Lastly, infrastructure development is also vital to both household livelihoods and economic activity[70]. We assessed the infrastructure occupation of residents in cities according to the per capita infrastructure area (I_{pc}):

$$I_{pc} = \frac{\text{Pop}}{\sum_{i=1}^{n} \text{Area}_\text{i}}, \tag{5}$$

where Pop represents the total population of the city, obtained from the Seventh National Population

Census, n denotes the number of specific infrastructure facilities, including healthcare and public service, and $Area_i$ represents the area of each facility.

Data Availability

The SinoBF-1[30] data of all 109 cities generated in this study have been deposited in the Zenodo database under accession code https://doi.org/10.5281/zenodo.17844789. The source data utilized in this study were collected from various platforms. The optical images are available at https://earth.google.com. The CNBH-10m building height dataset is available at https://zenodo.org/records/7827315. It is acknowledged that the SDGSAT-1 data are kindly provided by the International Research Center of Big Data for Sustainable Development Goals (CBAS) https://sdg.casearth.cn/en. The building footprint data, including the CN-OpenData and the East Asia Building Dataset, are available at https://doi.org/10.11888/Geogra.tpdc.271702 and https://zenodo.org/records/8174931. The Land use and AOI data used for constructing urban functional labels are retrieved from OpenStreetMap at https://www.openstreetmap.org/. The official government reports used for statistical validation are accessed from https://www.stats.gov.cn/sj/ndsj/2023/indexch.htm and https://www.mohurd.gov.cn/gongkai/fdzdgknr/sjfb/tjxx/jstjnj/index.html. The VGI data used in validation are provided through Amap at https://lbs.amap.com/api/javascript-api-v2. The 1-m land-cover map of China produced in our previous study is available at https://doi.org/10.5281/zenodo.7707461. The 100-meter gridded population dataset that was used to analyze housing inequality and infrastructure allocation is from China's seventh census dataset https://figshare.com/s/d9dd5f9bb1a7f4fd3734?file=43847643.

Code Availability

The full methodological framework[31], including the complete protocol, source code, and step-by-step implementation guidelines, is publicly available on GitHub at https://github.com/LiZhuoHong/SinoBF-1/. The repository provides comprehensive documentation, covering map utilization procedures, computation of multi-dimensional indicators, and reproducible workflows for building functional mapping.

References

1. Keith, M. *et al.* A new urban narrative for sustainable development. *Nat. Sustain.* **6**, 115–117 (2023).
2. Lu, Y. *et al.* Forty years of reform and opening up: China's progress toward a sustainable path. *Sci. advances* **5**, eaau9413 (2019).

3. Xu, F. *et al.* Using human mobility data to quantify experienced urban inequalities. *Nat. Hum. Behav.* 1–11 (2025).
4. Liu, X. *et al.* High-spatiotemporal-resolution mapping of global urban change from 1985 to 2015. *Nat. Sustain.* **3**, 564–570 (2020).
5. Yeh, A. G.-O. & Chen, Z. From cities to super mega city regions in china in a new wave of urbanisation and economic transition: Issues and challenges. *Urban Stud.* **57**, 636–654 (2020).
6. Chen, M., Gong, Y., Li, Y., Lu, D. & Zhang, H. Population distribution and urbanization on both sides of the hu huanyong line: Answering the premier's question. *J. Geogr. Sci.* **26**, 1593–1610 (2016).
7. Several opinions of the state council on further implementing the revitalization strategy of old industrial bases in northeast china and other regions (in Chinese). *The Bulletin of the State Council of the People's Republic of China.* https://www.gov.cn/gongbao/content/2009/content_1417927.htm (2009).
8. Naughton, B. The third front: defence industrialization in the chinese interior. *The China Q.* **115**, 351–386 (1988).
9. Pandey, B., Brelsford, C. & Seto, K. C. Infrastructure inequality is a characteristic of urbanization and others. *Proc. Natl. Acad. Sci.* **119**, e2119890119 (2022).
10. Arvidsson, M., Lovsjö, N. & Keuschnigg, M. Urban scaling laws arise from within-city inequalities. *Nat. Hum. Behav.* **7**, 365–374 (2023).
11. Brazil, N. Environmental inequality in the neighborhood networks of urban mobility in us cities. *Proc. Natl. Acad. Sci.* **119**, e2117776119 (2022).
12. Zhao, P., Li, J. & Zhang, M. Unequal roles of cities in the intercity healthcare system. *Nat. Cities* 1–12 (2025).
13. Sun, L., Chen, J., Li, Q. & Huang, D. Dramatic uneven urbanization of large cities throughout the world in recent decades. *Nat. communications* **11**, 5366 (2020).
14. Xu, Y., Olmos, L. E., Abbar, S. & González, M. C. Deconstructing laws of accessibility and facility distribution in cities. *Sci. advances* **6**, eabb4112 (2020).
15. Heris, M. P., Foks, N. L., Bagstad, K. J., Troy, A. & Ancona, Z. H. A rasterized building footprint dataset for the united states. *Sci. data* **7**, 207 (2020).
16. Wang, H. The role of informal ruralization within china's rapid urbanization. *Nat. Cities* **1**, 205–215 (2024).
17. Hou, Z. *et al.* War city profiles drawn from satellite images. *Nat. Cities* **1**, 359–369 (2024).
18. Wang, L., Saiz, A. & Li, W. Natural fragmentation increases urban density but impedes transportation and city growth worldwide. *Nat. Cities* **1**, 642–653 (2024).
19. Chen, T.-H. K. *et al.* Higher depression risks in medium-than in high-density urban form across denmark. *Sci. advances* **9**, eadf3760 (2023).
20. Zheng, H., Zhang, R., Yin, X. & Wu, J. Unused housing in urban china and its carbon emission impact. *Nat. Commun.* **16**, 1985 (2025).
21. Che, Y. *et al.* 3d-globfp: the first global three-dimensional building footprint dataset. *Earth Syst. Sci. Data* **16**, 5357–5374 (2024).
22. Esch, T. *et al.* World settlement footprint 3d-a first three-dimensional survey of the global building stock. *Remote. sensing environment* **270**, 112877 (2022).
23. Zhang, Y., Zhao, H. & Long, Y. Cmab: A multi-attribute building dataset of china. *Sci. Data* **12**, 430 (2025).

24. Weiss, D. J. *et al.* A global map of travel time to cities to assess inequalities in accessibility in 2015. *Nature* **553**, 333–336 (2018).

25. Pandey, B., Brelsford, C. & Seto, K. C. Rising infrastructure inequalities accompany urbanization and economic development. *Nat. Commun.* **16**, 1193 (2025).

26. Bruno, M., Monteiro Melo, H. P., Campanelli, B. & Loreto, V. A universal framework for inclusive 15-minute cities. *Nat. Cities* **1**, 633–641 (2024).

27. Rocha, A. D. *et al.* Unprivileged groups are less served by green cooling services in major european urban areas. *Nat. Cities* **1**, 424–435 (2024).

28. Meehan, K., Jurjevich, J. R., Everitt, L., Chun, N. M. & Sherrill, J. Urban inequality, the housing crisis and deteriorating water access in us cities. *Nat. Cities* **2**, 93–103 (2025).

29. Wu, X., Xu, X., Chen, G., Liao, W. & Liu, X. Exploring urban building space provision and inequality: A three-dimensional perspective on Chinese cities toward sustainable development goals. *Sustain. Cities Soc.* **102**, 105202 (2024).

30. Li, Z. *et al.* Satellite mapping of every building's function in urban china reveals deep built environment disparities. Zenodo repository, 10.5281/zenodo.17844788 (2025).

31. Li, Z. *et al.* Satellite mapping of every building's function in urban china reveals deep built environment disparities. GitHub repository, 10.5281/zenodo.17851286 (2025).

32. China statistical yearbook (in Chinese). *National Bureau of Statistics of China.* https://www.stats.gov.cn/sj/ndsj/2023/indexch.htm (2023).

33. China urban-rural construction statistical yearbook (in Chinese). *Ministry of Housing and Urban-Rural Development of the People's Republic of China.* https://www.mohurd.gov.cn/gongkai/fdzdgknr/sjfb/tjxx/jstjnj/index.html (2023).

34. Lin, B. & Wang, C. Does industrial relocation affect regional carbon intensity? evidence from china's secondary industry. *Energy Policy* **173**, 113339 (2023).

35. Huang, Y. & Zhang, M. A study on the allocation of special education resources in china. *Int. J. Humanit. Soc. Sci* **6**, 14–22 (2019).

36. Huang, Z., He, C. & Zhu, S. Do china's economic development zones improve land use efficiency? the effects of selection, factor accumulation and agglomeration. *Landsc. urban Plan.* **162**, 145–156 (2017).

37. Shi, Y. & Liu, D. Excessive urbanization and rejuvenation in the metropolitan city center in shanghai, china. *J. Urban Plan. Dev.* **144**, 05018020 (2018).

38. Action plan for promoting high quality construction of national developing zones(in Chinese). *National Development and Reform Commission of China.* https://www.gov.cn/lianbo/bumen/202403/content_6939721.htm (2024).

39. Fan, J. & Zou, B. Industrialization from scratch: The "construction of third front" and local economic development in china's hinterland. *J. Dev. Econ.* **152**, 102698 (2021).

40. Ye, P. *et al.* National-scale 1-km maps of hospital travel time and hospital accessibility in china. *Sci. Data* **11**, 1130 (2024).

41. Zhao, J., Tang, Y., Zhu, X. & Zhu, J. National environmental monitoring and local enforcement strategies. *Nat. Cities* **2**, 58–69 (2025).

42. Gao, T. *et al.* The impact of new western land and sea corridor development on port deep hinterland transport service and route selection. *Ocean. & Coast. Manag.* **247**, 106910 (2024).

43. Zhou, Y. *et al.* Satellite mapping of urban built-up heights reveals extreme infrastructure gaps and inequalities in the global south. *Proc. Natl. Acad. Sci.* **119**, e2214813119 (2022).

44. Zhang, X. *et al.* Underload city conceptual approach extending ghost city studies. *npj Urban Sustain.* **2**, 15 (2022).

45. Housing affordability index of 135 large and medium sized cities in china from 2010 to 2022 (in Chinese). *National Development Institute of Renmin University of China.* http://nads.ruc.edu.cn/zkcg/ndyjbg/3c417101af10422b998f1a5e82bb3e28.htm (2023).

46. Chinese general social survey (in Chinese). *Renmin University of China.* http://cgss.ruc.edu.cn/ (2022).

47. Han, C., Lu, B., Zheng, J., Yu, D. & Zheng, S. Research on multiscale openstreetmap in china: data quality assessment with ewm-topsis and gdp modeling. *Geo-spatial Inf. Sci.* **28**, 1316–1340 (2025).

48. Shang, H. *et al.* Osm land use data quality and its association with city-level socioeconomic conditions in china. *Environ. Plan. B: Urban Anal. City Sci.* **0**, 23998083251341667 (0).

49. Herfort, B., Lautenbach, S., Porto de Albuquerque, J., Anderson, J. & Zipf, A. A spatio-temporal analysis investigating completeness and inequalities of global urban building data in openstreetmap. *Nat. Commun.* **14**, 3985 (2023).

50. Pulighe, G., Baiocchi, V. & Lupia, F. Horizontal accuracy assessment of very high resolution google earth images in the city of rome, italy. *Int. J. Digit. Earth* **9**, 342–362 (2016).

51. Wu, W.-B. *et al.* A first chinese building height estimate at 10 m resolution (cnbh-10 m) using multi-source earth observations and machine learning. *Remote. Sens. Environ.* **291**, 113578 (2023).

52. Guo, H. *et al.* Sdgsat-1: the world's first scientific satellite for sustainable development goals. *Sci. Bull* **68**, 34–38 (2023).

53. Li, C., Chen, F., Wang, N., Yu, B. & Wang, L. Sdgsat-1 nighttime light data improve village-scale built-up delineation. *Remote. Sens. Environ.* **297**, 113764 (2023).

54. Wu, B., Wang, Y., Huang, H., Liu, S. & Yu, B. Potential of sdgsat-1 nighttime light data in extracting urban main roads. *Remote. Sens. Environ.* **315**, 114448 (2024).

55. Li, Z. *et al.* Sinolc-1: the first 1 m resolution national-scale land-cover map of china created with a deep learning framework and open-access data. *Earth Syst. Sci. Data* **15**, 4749–4780 (2023).

56. Zhang, Z. *et al.* Vectorized rooftop area data for 90 cities in china. *Sci. Data* **9**, 66 (2022).

57. Shi, Q. *et al.* The last puzzle of global building footprints—mapping 280 million buildings in east asia based on vhr images. *J. Remote. Sens.* **4**, 0138 (2024).

58. Chen, Z. *et al.* Public transport accessibility in villages in and around major chinese cities. *Nat. Cities* **2**, 749–758 (2025).

59. Zhong, Y. *et al.* Open-source data-driven urban land-use mapping integrating point-line-polygon semantic objects: A case study of chinese cities. *Remote. Sens. Environ.* **247**, 111838 (2020).

60. Li, Z., He, W., Li, J., Lu, F. & Zhang, H. Learning without exact guidance: Updating large-scale high-resolution land cover maps from low-resolution historical labels. In *Proceedings of the IEEE/CVF Conference on Computer Vision and Pattern Recognition*, 27717–27727 (2024).

61. Li, Z. *et al.* Breaking the resolution barrier: A low-to-high network for large-scale high-resolution land-cover mapping using low-resolution labels. *ISPRS J. Photogramm. Remote. Sens.* **192**, 244–267 (2022).

62. He, K., Gkioxari, G., Dollar, P. & Girshick, R. Mask r-cnn. In *Proceedings of the IEEE International Conference on Computer Vision (ICCV)* (2017).

63. Li, X. *et al.* Mapping global urban boundaries from the global artificial impervious area (gaia) data. *Environ. Res. Lett.* **15**, 094044 (2020).

64. Hu, S., Ge, Y., Liu, M., Ren, Z. & Zhang, X. Village-level poverty identification using machine learning, high-resolution images, and geospatial data. *Int. J. Appl. Earth Obs. Geoinformation* **107**, 102694, https://doi.org/10.1016/j.jag.2022.102694 (2022).

65. Lindsay, J. The whitebox geospatial analysis tools project and open-access gis. In *Proceedings of the GIS research UK 22nd annual conference, The University of Glasgow*, 16–18 (2014).

66. Technical guidelines for community living circle planning. *Ministry of Natural Resources of the People's Republic of China.* https://www.beijing.gov.cn/zhengce/zhengcefagui/qtwj/202204/t20220407_2668427.html (2021).

67. Pozoukidou, G. & Chatziyiannaki, Z. 15-minute city: Decomposing the new urban planning eutopia. *Sustainability* **13** (2021).

68. Guan, C., Wang, Y., Keith, M., Li, Y. & Cao, G. Does local planning of fast-growing medium-sized towns lead to higher urban intensity or to sprawl? Cases from Zhejiang Province. *Cities* **130**, 103869 (2022).

69. Ghosh, T., Coscieme, L., Anderson, S. J. & Sutton, P. C. Building volume per capita (bvpc): A spatially explicit measure of inequality relevant to the sdgs. *Front. Sustain. Cities* **2**, 37 (2020).

70. Stokes, E. C. & Seto, K. C. Characterizing urban infrastructural transitions for the sustainable development goals using multi-temporal land, population, and nighttime light data. *Remote. Sens. Environ.* **234**, 111430 (2019).

Acknowledgements

This work was supported by the National Natural Science Foundation of China (T2525018 to H.Z., 42230108 to L.Z., 42271370 to W.H., and 42201377 to T.H.) and the Open Fund of State Key Laboratory of Information Engineering in Surveying, Mapping and Remote Sensing, Wuhan University (24R06 to T.H.).

Author Contributions Statement

H.Z. conceived and supervised the whole project. Z.L. designed and organized the mapping framework of this study. Z.L., L.L., and T.H., performed data analysis and interpretation. H.Z., W.H., and T.H. supervised the Methods sections. Z.L., L.L., and M.C. contributed to producing the building function map. Z.H., L.L., M.C., T.H., T.Q., and H.Z. conducted the multi-dimensional assessments of inequality. Z.L., H.Z., L.L., T.H., T.Q., W.H., and L.Z. contributed to the result discussion and overall analysis. Z.L., H.Z., L.L., T.H., M.C., W.H., T.Q., and L.Z. wrote and revised the manuscript.

Competing Interests Statement

The authors declare no competing interests.

Figure. 1: Building function mapping and distribution across cities. **(a)** Workflow for building function classification and a representative output for Beijing. Multi-modal satellite data that captured optical appearance, building height, and nighttime light intensity were integrated to classify buildings into eight functional categories. The legend on the right shows the function types and corresponding color codes. **(b)** and **(c)** Total number, density, and functional composition of buildings across 109 cities, grouped by five development tiers. The tier system reflects China's economic and administrative hierarchy, with Tier 1 cities representing the most economically developed, and Tier 5 cities representing smaller, less-developed municipalities. Clip-art elements were created using © Icograms https://icograms.com/. Maps data © 2025 Google.

Figure. 2: Multi-dimensional assessment of built environment disparities in 109 cities across China. Each row presents three indicators corresponding to one of the three dimensions at the national scale; legends are provided in the bottom-left corner of each map. **(a)** Urbanization intensity, represented by building height, building density, and nighttime light intensity. They serve as indicators of urban development and concentration. **(b)** Facility accessibility, measured as the travel time from each residential building to the nearest educational, healthcare, and public service facility. **(c)** Infrastructure sufficiency, assessed by neighborhood amenity diversity (Shannon entropy), inequality in residential capacity allocation (Gini coefficient), and per capita infrastructure occupation. These indicators reflect the diversity, equity, and adequacy of the residential built environment. Basemap data © 2025 Esri, USGS, World Hillshade, used under Duke University ArcGIS Pro license.

Figure. 3: Built environment disparities across city tiers: urbanization intensity and facility accessibility. **(a)** Left: distribution of building heights across five city tiers, with the mode value labeled for each tier (as the peak of the curve). Right: statistical comparison of building density and nighttime light intensity among city tiers. **(b)** Cumulative accessibility curves showing travel time from residential buildings to the nearest educational, healthcare, and public service facilities. **(c)** Population distribution and accessibility maps of representative cities from each tier.

Figure. 4: Built environment disparity across city tiers and geographic regions: infrastructure sufficiency. **(a)** Assessment of neighborhood amenity diversity across 109 cities, categorized into four quadrants: I—high diversity and high availability; II—low diversity, high availability; III—high diversity, low availability; IV—low diversity and low availability. At the top, T1–T5 indicate cities in Tier 1–5. Regional abbreviations are as follows: C, Central; E, East; S, South; N, North; NW, Northwest; NE, Northeast; SW, Southwest. **(b)** Violin plots of housing inequality indices measured by the Gini coefficient between housing volume and population, shown by city tier (top) and geographic region (bottom). Whiskers and red lines indicate maximum, minimum, and median values. **(c)** and **(d)** Per capita public infrastructure provision (public services and healthcare, respectively), shown as histograms where each bar represents one city. Bar width reflects cumulative population size, and representative cities are labeled.

Figure. 5: The overall assessment of urban disparities across city tiers, geographic regions, and within-city zones. **(a)** Zoning approach applied to Beijing, delineating the three divided zones based on administrative boundaries and functional roles; the same method was used for all study cities. **(b)** and **(c)** Average facility accessibility (b) and infrastructure sufficiency (c) across the three zones in 109 cities. **(d)** Distribution of composite disparities scores across city tiers and geographic regions. Scores are based on normalized values (0–10) for six building-level indicators (three per dimension in e). Each grid cell represents the average score for all cities in the corresponding tier–region combination. **(e)** The six indicators used in the overall assessment, grouped by dimension: facility accessibility (top three) and infrastructure sufficiency (bottom three). Clip-art elements were created using © Icograms https://icograms.com/. Basemap data © 2025 Esri, USGS, World Hillshade, used under Duke University ArcGIS Pro license.

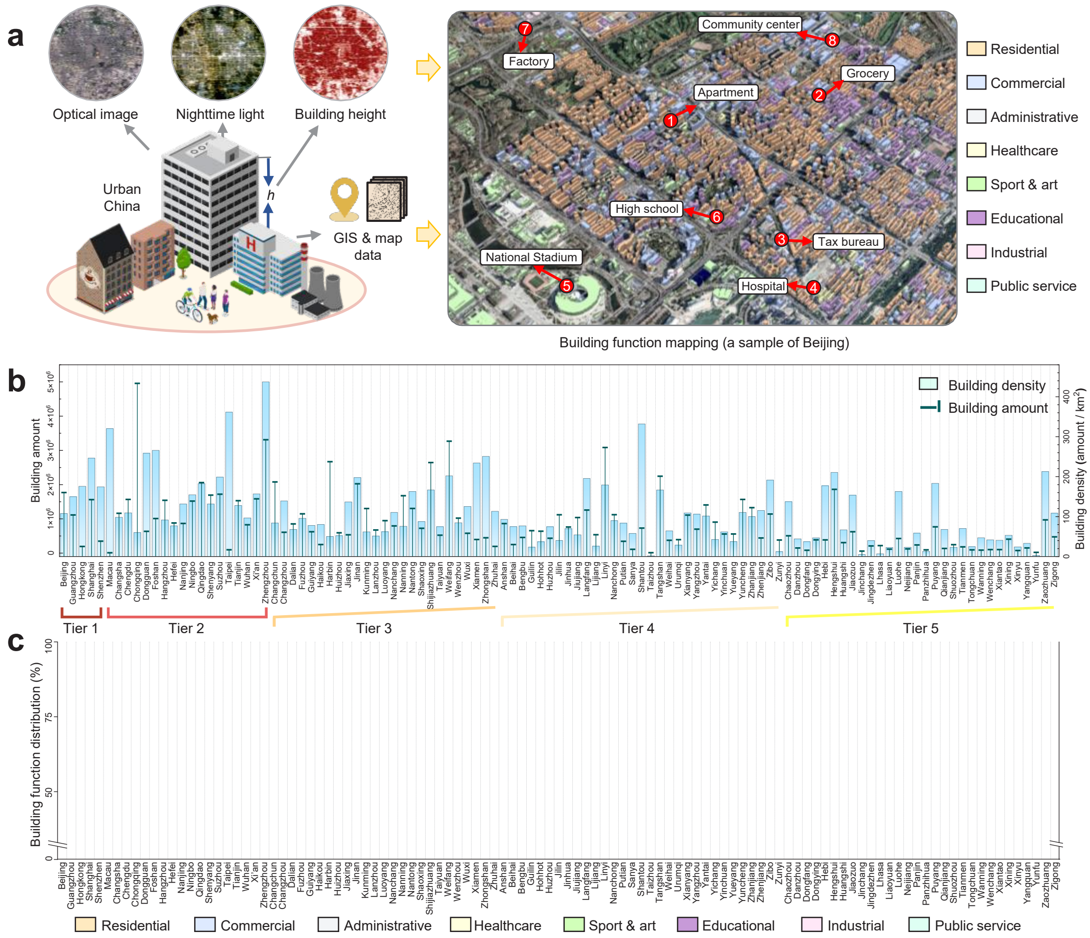
a
Optical image
Nighttime light
Building height
Urban China
h
GIS & map data
Community center
Factory
Grocery
Apartment
High school
Tax bureau
National Stadium
Hospital
Residential
Commercial
Administrative
Healthcare
Sport & art
Educational
Industrial
Public service
Building function mapping (a sample of Beijing)
b
Building amount
Building density (amount / km²)
Building density
Building amount
Tier 1
Tier 2
Tier 3
Tier 4
Tier 5
c
Building function distribution (%)
Residential
Commercial
Administrative
Healthcare
Sport & art
Educational
Industrial
Public service

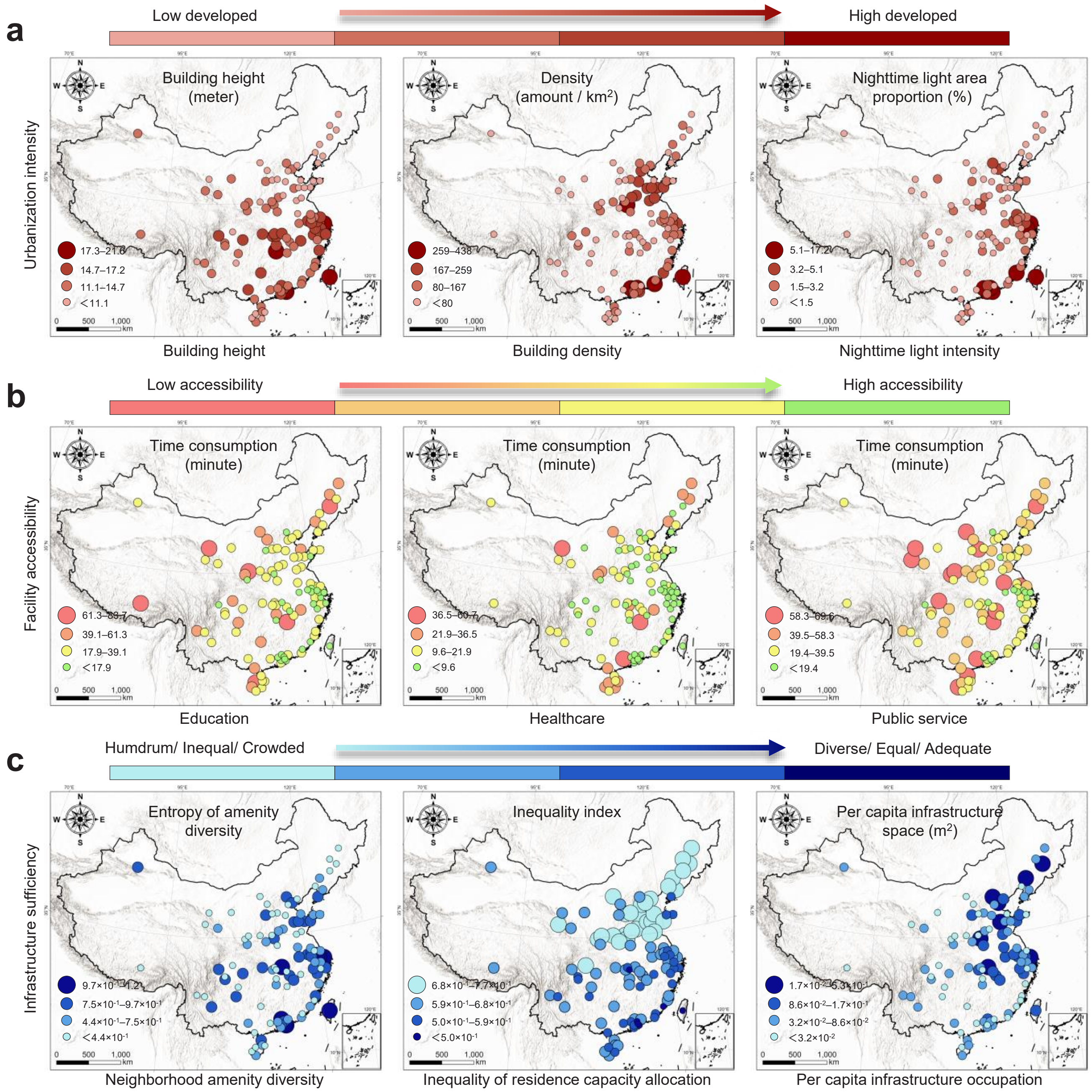
a
Low developed
High developed
Urbanization intensity
Building height (meter)
14.7–17.2
11.1–14.7
<11.1
Building height
Density (amount / km²)
167–259
80–167
<80
Building density
Nighttime light area proportion (%)
3.2–5.1
1.5–3.2
<1.5
Nighttime light intensity
b
Low accessibility
High accessibility
Facility accessibility
Time consumption (minute)
39.1–61.3
17.9–39.1
<17.9
Education
21.9–36.5
9.6–21.9
<9.6
Healthcare
39.5–58.3
19.4–39.5
<19.4
Public service
c
Humdrum/ Inequal/ Crowded
Diverse/ Equal/ Adequate
Infrastructure sufficiency
Entropy of amenity diversity
7.5×10⁻¹–9.7×10⁻¹
4.4×10⁻¹–7.5×10⁻¹
<4.4×10⁻¹
Neighborhood amenity diversity
Inequality index
5.9×10⁻¹–6.8×10⁻¹
5.0×10⁻¹–5.9×10⁻¹
<5.0×10⁻¹
Inequality of residence capacity allocation
Per capita infrastructure space (m²)
8.6×10⁻²–1.7×10⁻¹
3.2×10⁻²–8.6×10⁻²
<3.2×10⁻²
Per capita infrastructure occupation
0 500 1,000 km

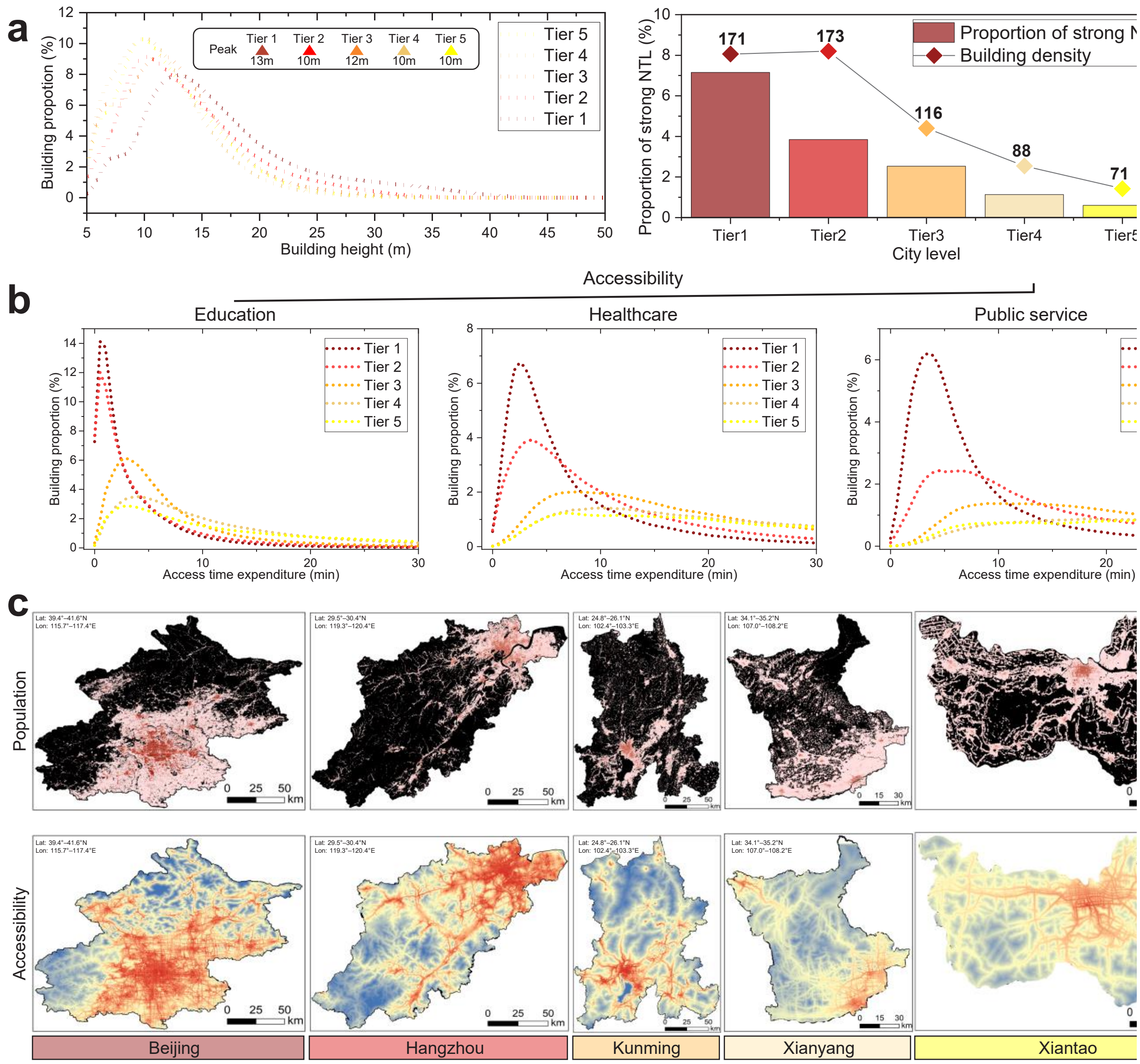

a
Building propotion (%)
Building height (m)
Peak
Tier 1 13m
Tier 2 10m
Tier 3 12m
Tier 4 10m
Tier 5 10m
Tier 5
Tier 4
Tier 3
Tier 2
Tier 1
Proportion of strong NTL (%)
Proportion of strong N
Building density
171
173
116
88
71
Tier1
Tier2
Tier3
Tier4
Tier5
City level
b
Accessibility
Education
Healthcare
Public service
Building proportion (%)
Access time expenditure (min)
c
Population
Accessibility
Beijing
Hangzhou
Kunming
Xianyang
Xiantao

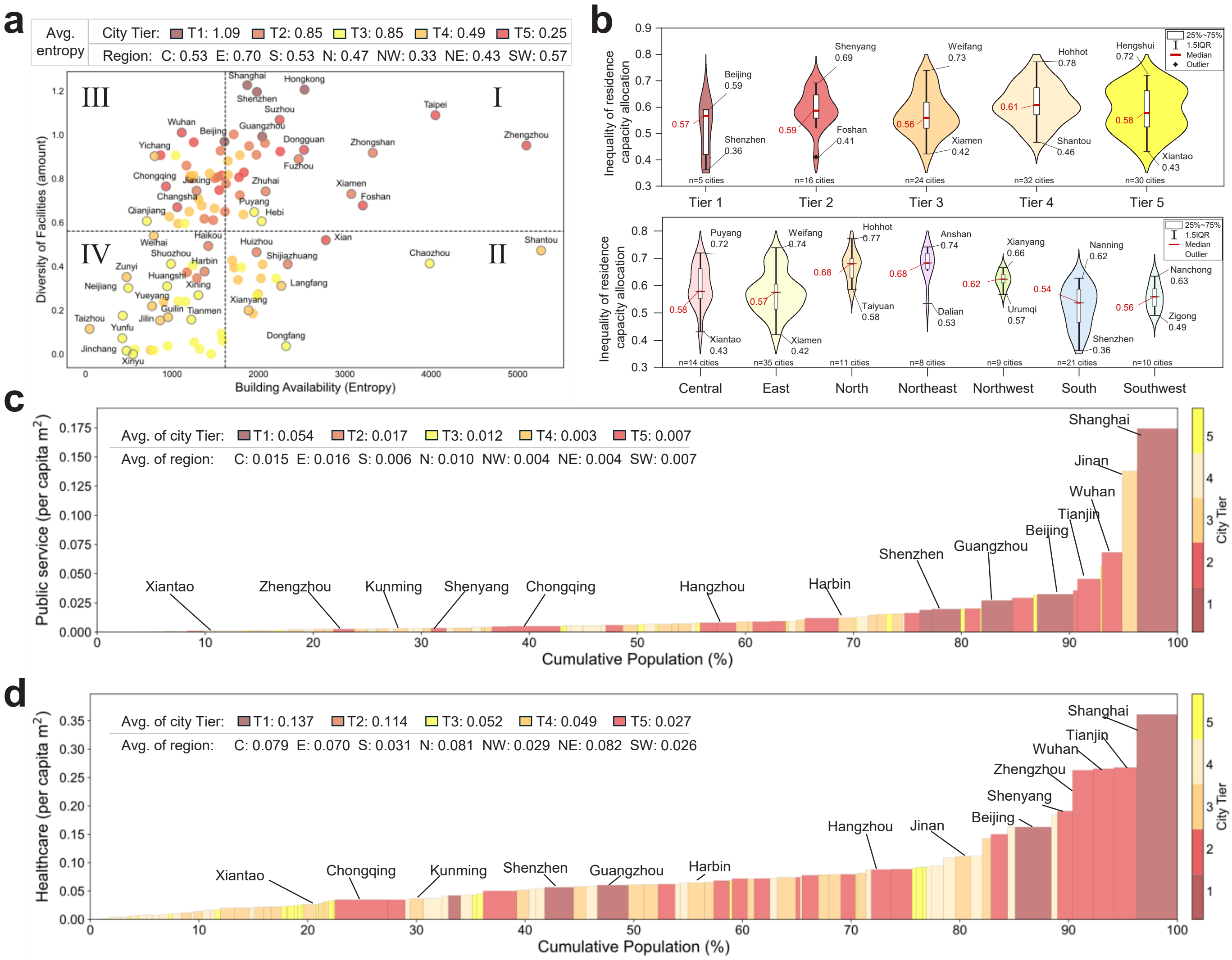
a
Avg. entropy
City Tier: T1: 1.09 T2: 0.85 T3: 0.85 T4: 0.49 T5: 0.25
Region: C: 0.53 E: 0.70 S: 0.53 N: 0.47 NW: 0.33 NE: 0.43 SW: 0.57
Diversity of Facilities (amount)
Building Availability (Entropy)
I
II
III
IV
b
Inequality of residence capacity allocation
Tier 1
Tier 2
Tier 3
Tier 4
Tier 5
Central
East
North
Northeast
Northwest
South
Southwest
25%~75%
1.5IQR
Median
Outlier
c
Avg. of city Tier: T1: 0.054 T2: 0.017 T3: 0.012 T4: 0.003 T5: 0.007
Avg. of region: C: 0.015 E: 0.016 S: 0.006 N: 0.010 NW: 0.004 NE: 0.004 SW: 0.007
Public service (per capita m^2)
Cumulative Population (%)
City Tier
d
Avg. of city Tier: T1: 0.137 T2: 0.114 T3: 0.052 T4: 0.049 T5: 0.027
Avg. of region: C: 0.079 E: 0.070 S: 0.031 N: 0.081 NW: 0.029 NE: 0.082 SW: 0.026
Healthcare (per capita m^2)
Cumulative Population (%)
City Tier

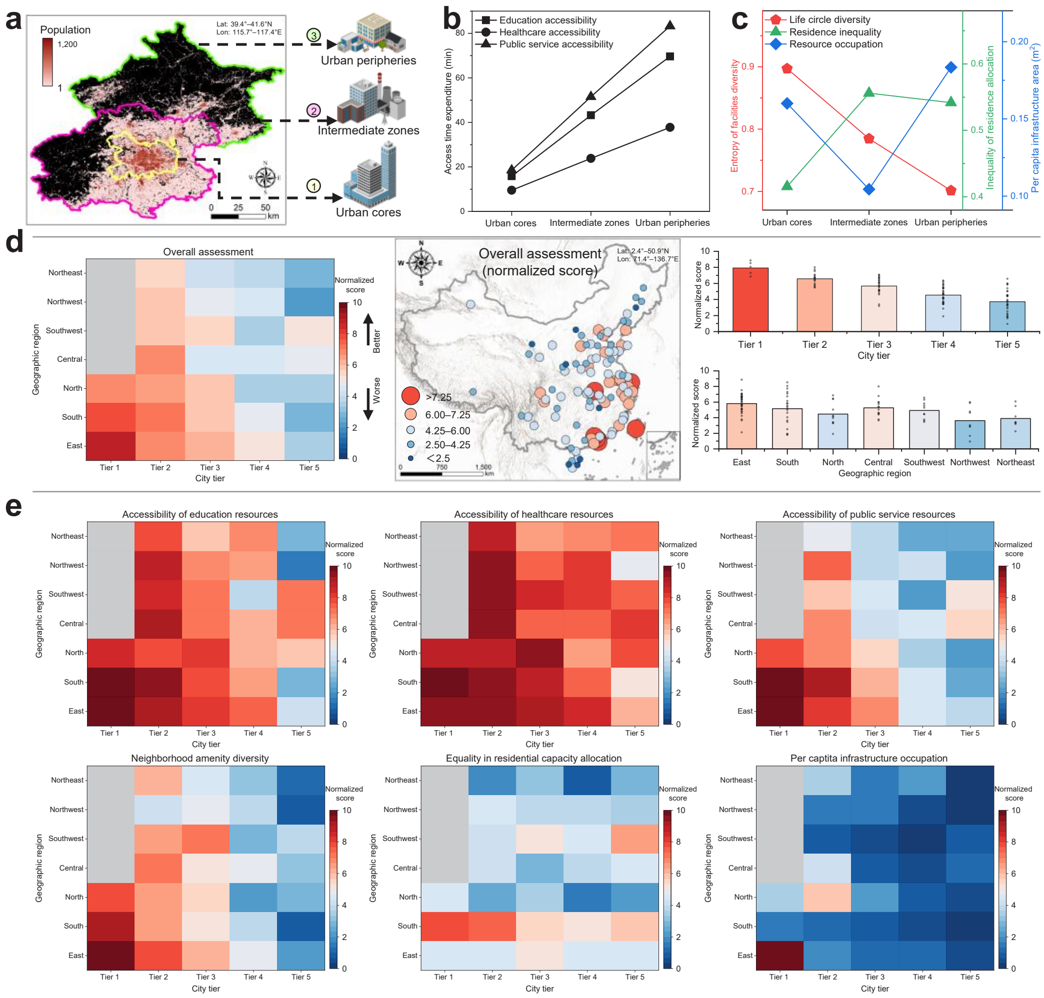

a
Population
Urban peripheries
Intermediate zones
Urban cores
b
Education accessibility
Healthcare accessibility
Public service accessibility
Access time expenditure (min)
Urban cores
Intermediate zones
Urban peripheries
c
Life circle diversity
Residence inequality
Resource occupation
Entropy of facilities diversity
Inequality of residence allocation
Per capita infrastructure area (m²)
d
Overall assessment
Overall assessment (normalized score)
Geographic region
City tier
Normalized score
Better
Worse
e
Accessibility of education resources
Accessibility of healthcare resources
Accessibility of public service resources
Neighborhood amenity diversity
Equality in residential capacity allocation
Per captita infrastructure occupation